

Internal Chemistry of the Pure and Chemically Substituted Quadruple Perovskites $\text{Ln}'\text{Ln}''\text{Ba}_2\text{Cu}_2\text{Ti}_2\text{O}_{11}$ ($\text{Ln}'\text{Ln}'' = \text{LaY}$ or NdDy)

P. A. Salvador,^{†,‡,§} T. O. Mason,^{†,‡} K. Otszchi,^{‡,||} K. B. Greenwood,^{‡,||,⊥}
K. R. Poeppelmeier,^{*,‡} and B. Dabrowski[#]

Contribution from the Departments of Materials Science and Engineering and Chemistry and Science and Technology Center for Superconductivity, Northwestern University, Evanston, Illinois 60208-3108, and Department of Physics and Science and Technology Center for Superconductivity, Northern Illinois University, DeKalb, Illinois 60115

Received November 12, 1996[⊗]

Abstract: Important features of the internal chemistry of the quadruple perovskite family of layered cuprates, such as solid solution behavior, stable defect species, and oxidation behavior, have been investigated by structural and physical property measurements and related to the inner architecture of these potential superconductors. In-situ high-temperature (650–800 °C) electrical conductivity and Seebeck coefficient measurements have been performed, in various oxygen partial pressures, on pure and chemically substituted $\text{Ln}'\text{Ln}''\text{Ba}_2\text{Cu}_2\text{Ti}_2\text{O}_{11}$ ($\text{Ln}'\text{Ln}'' = \text{LaY}$ or NdDy) compounds. The electrical properties display transitions from dual carrier (intrinsic) semiconductivity to extrinsically doped p-type semiconductivity as a function of chemical composition, temperature, and oxygen pressure. The exclusion of interstitial oxygen defects between the copper–oxygen double layers, as evidenced in the weak oxygen partial pressure dependence of the electrical properties in the $\text{LaYBa}_2\text{Cu}_2\text{Ti}_2\text{O}_{11}$ systems, is directly related to the A-site order and is an important step toward achieving superconductivity by preserving the structural integrity of the CuO_2^{2-} planes. The electrical properties of the NdDy system, however, are strong functions of the oxygen partial pressure, indicating that oxygen defects play an important role in determining their properties. Oxidation of the latter compound has been achieved, and underdoped metallic behavior reminiscent of known superconductors has been observed at low temperatures (100–300 K). Jonker analysis of the electrical properties of the highly oxidized material further illustrates the similarity of the transport behavior of the quadruple perovskites to superconducting cuprates. A combination of synthesis and annealing methods which allow for both increased substitution levels and carrier concentrations should lead to superconductivity in the ordered-lanthanide quadruple perovskites.

Introduction

It is widely recognized that high- T_c cuprates contain CuO_2^{2-} sheets interleaved by inorganic layers and that to realize superconductivity an appropriate concentration of charge carriers must be introduced, thereby oxidizing or reducing the CuO_2^{2-} sheets. The amount and type of stable charge carriers are controlled by the internal chemistry such as oxygen intercalation, solid solution limits, and stable defect species. Because these chemical factors are directly related to the observed atomic structure and macroscopic properties, in-situ equilibrium physical property measurements, combined with crystal structural data, provide invaluable insights into the complex solid state chemistry of cuprate superconductors. We have been investigating the electronic/structural aspects of both superconducting and non-superconducting layered cuprates in order to discern their fundamental differences. Herein, we report on several pure and chemically substituted quadruple perovskites, of the nominal

stoichiometry $\text{Ln}'\text{Ln}''\text{Ba}_2\text{Cu}_2\text{Ti}_2\text{O}_{11\pm\delta}$ ($\text{Ln}'\text{Ln}'' = \text{LaY}$, NdDy). The normal state properties and absence of superconductivity are directly related to several features of the inner architecture and internal chemistry of quadruple perovskites; however, the potential for superconductivity in these materials is demonstrated and discussed.

The structure of the quadruple perovskites is depicted in Figure 1 and was first reported for the material $\text{La}_2\text{Ba}_2\text{Cu}_2\text{Sn}_2\text{O}_{11}$.¹ Several research groups achieved the replacement of tin by titanium for the stoichiometries $\text{Ln}_2\text{Ba}_2\text{Cu}_2\text{Ti}_2\text{O}_{11}$ ($\text{Ln} = \text{La–Tb}$).^{2–6} The structure can be described as an oxygen-deficient perovskite where concerted order of the cations and the oxygen vacancies results in the familiar double square pyramidal layers of copper–oxygen polyhedra, as in $\text{YBa}_2\text{Cu}_3\text{O}_7$ (YBCO , $T_c = 92$ K),^{7,8} $\text{YSr}_2\text{Cu}_2\text{GaO}_7$ ($T_c = 40$ K),^{9,10} and $\text{La}_2\text{CaCu}_2\text{O}_6$ ($T_c = 60$ K).^{11,12} The copper–oxygen sheets are

* Author to whom correspondence should be addressed.

† Department of Materials Science and Engineering, Northwestern University.

‡ Science and Technology Center for Superconductivity, Northwestern University.

§ Present address: Laboratoire CRISMAT, ISMRA, Université de Caen, Bd du Maréchal Juin, 14050, Caen cedex, France.

|| Department of Chemistry, Northwestern University.

⊥ Present address: Department of Chemistry, North Carolina State University, Raleigh NC 27695-8204.

Northern Illinois University.

⊗ Abstract published in *Advance ACS Abstracts*, March 1, 1997.

(1) Anderson, M. T.; Poeppelmeier, K. R.; Zhang, J. P.; Fan, H.-J.; Marks, L. D. *Chem. Mater.* **1992**, *4*, 1305–1313.

(2) Gormezano, A.; Weller, M. T. *J. Mater. Chem.* **1993**, *3*, 979–982.

(3) Gormezano, A.; Weller, M. T. *J. Mater. Chem.* **1993**, *3*, 771–772.

(4) Palacín, M. R.; Fuertes, A.; Casañ-Pastor, N.; Gómez-Romero, P. *Adv. Mater.* **1994**, *6*, 54–57.

(5) Greenwood, K. B.; Anderson, M. T.; Poeppelmeier, K. R.; Novikov, D. L.; Freeman, A. J.; Dabrowski, B.; Gramsch, S. A.; Burdett, J. K. *Physica C* **1994**, *235–240*, 349–350.

(6) Palacín, M. R.; Krumeich, F.; Caldés, M. T.; Gómez-Romero, P. *J. Solid State Chem.* **1995**, *117*, 213–216.

(7) Wu, M. K.; Ashburn, J. R.; Torng, C. J.; Hor, P. H.; Meng, R. L.; Gao, L.; Huang, Z. J.; Wang, Y. Q.; Chu, C. W. *Phys. Rev. Lett.* **1987**, *58*, 908–910.

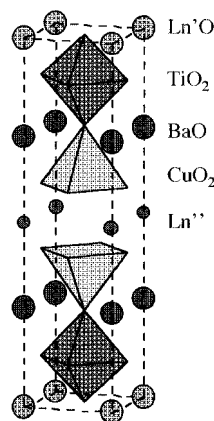


Figure 1. Polyhedral representation of the quadruple perovskite, $\text{Ln}'\text{Ln}''\text{Ba}_2\text{Cu}_2\text{Ti}_2\text{O}_{11}$, structure. The copper cations sit at the center of the square pyramids, titanium cations at the center of the octahedra, and oxygen at the vertices of the polyhedra. The Ln' , Ln'' , and Ba cations correspond to the small light spheres, large light spheres, and large dark spheres, respectively.

interleaved by a double layer of corner-sharing octahedrally coordinated cations (perovskite blocks— ABO_3) resulting in a tetragonal cell of approximate dimensions $1a_p \times 1a_p \times 4a_p$ (a_p = cubic perovskite cell dimension). Compared to the aforementioned superconducting systems, the double-octahedra blocking layer in the quadruple perovskites results in a large separation between conducting copper–oxygen layers. Thus, comparisons between similarly doped quadruple perovskites and known superconducting systems would provide insight concerning the importance of c -axis coupling in superconducting cuprates.

The absence of superconductivity in the quadruple perovskites has been partly attributed to the long Cu–O in-plane bond lengths (≈ 1.95 Å for $\text{Tb}_2\text{Ba}_2\text{Cu}_2\text{Ti}_2\text{O}_{11}$ ⁶ and $\text{Gd}_2\text{Ba}_2\text{Cu}_2\text{Ti}_2\text{O}_{11}$ ³ and ≈ 2.00 Å in $\text{La}_2\text{Ba}_2\text{Cu}_2\text{Sn}_2\text{O}_{11}$ ¹) which are 0.01–0.06 Å larger than known hole-type superconductors. In-situ high-temperature electrical conductivity and thermopower measurements of several of these materials ($\text{La}_2\text{Ba}_2\text{Cu}_2\text{Sn}_2\text{O}_{11}$, $\text{La}_2\text{Ba}_2\text{Cu}_2\text{Ti}_2\text{O}_{11}$, and $\text{Eu}_2\text{Ba}_2\text{Cu}_2\text{Ti}_2\text{O}_{11}$) demonstrated the similarity of their transport properties to those of the superconducting layered cuprates and showed that low carrier concentrations were predominantly responsible for the absence of superconductivity.¹³ Band structure calculations confirmed that the electronic structures of the quadruple perovskite materials were extremely similar to other high- T_c cuprates (having extended two-dimensional Cu–O bands crossing the Fermi level and van Hove singularities below the Fermi level).¹⁴ These observations imply that there is no fundamental physical impediment, such as long in-plane Cu–O bond lengths, to obtaining superconductivity in the quadruple perovskites, and that a complete understanding of these materials has yet to be attained.

(8) Beno, M. A.; Soderholm, L.; D. W. Capone, I.; Hinks, D. G.; Jorgensen, J. D.; Grace, J. D.; Schuller, I. K.; Segre, C. U.; Zhang, K. *Appl. Phys. Lett.* **1987**, *51*, 57–59.

(9) Vaughey, J. T.; Thiel, J. P.; Hastly, E. F.; Groenke, D. A.; Stern, C. L.; Poeppelmeier, K. R.; Dabrowski, B.; Hinks, D. G.; Mitchell, A. W. *Chem. Mater.* **1991**, *3*, 935–940.

(10) Roth, G.; Adelman, P.; Hegar, G.; Knitter, R.; Wolf, T. *J. Phys. I* **1991**, *1*, 721.

(11) Cava, R. J.; Batlogg, B.; Dover, R. B. v.; Krajewski, J. J.; Waszczak, J. V.; Fleming, R. M.; Peck, W. F., Jr.; Rupp, L. W., Jr.; Marsh, P.; James, A. C. W. P.; Schneemeyer, L. F. *Nature* **1990**, *345*, 602–604.

(12) Kinoshita, K.; Izumi, F.; Yamada, T.; Asano, H. *Phys. Rev. B* **1992**, *45*, 5558–5563.

(13) Salvador, P. A.; Shen, L.; Mason, T. O.; Greenwood, K. B.; Poeppelmeier, K. R. *J. Solid State Chem.* **1995**, *119*, 80–89.

(14) Novikov, D. L.; Freeman, A. J.; Poeppelmeier, K. R. *Phys. Rev. B* **1996**, *53*, 9448–9452.

(15) Jennings, R. A.; Greaves, C. *Physica C* **1994**, *235–240*, 989–990.

An important chemical feature of the quadruple perovskites is the occurrence of anionic defects, either as acceptor doping species or compensation mechanisms to substituted cations (depending on the type and structural location of the defect). The dependence of the equilibrium electrical conductivity on the partial pressure of oxygen for the quadruple perovskites at elevated temperatures was explained on the basis of doubly charged oxygen interstitials residing between the $(\text{CuO}_2)^{2-}$ sheets.¹³ While it was demonstrated that these anionic defects did indeed oxidize the copper oxygen planes, the extent of doping was insufficient (even at high oxygen pressures) to induce superconductivity.¹³ Moreover, the structural location of these defects may be deleterious to superconductivity. Band structure calculations showed that the two-dimensional character of the Fermi level in the quadruple perovskite is destroyed when extra oxygen is incorporated between the copper–oxygen square pyramids.¹⁴ Several doping studies have shown that regardless of the doping strategy adopted^{1,15–19} a significant increase in carrier concentrations is not achieved. Recent investigations by the authors^{5,16,19} and others^{15–17,19} have shown that anion vacancies compensate successful acceptor substitutions, leaving the copper–oxygen planes underdoped. Therefore, strict control of the inner architecture will be required if optimal doping concentrations are to be realized. In addition, the chemical factors which restrict oxidation in these materials are important to understand in order to realize superconductivity in this structure and other related layered cuprates.

Recently, we reported several new materials belonging to the quadruple perovskite family of the stoichiometries $\text{Ln}'\text{Ln}''\text{Ba}_2\text{Cu}_2\text{Ti}_2\text{O}_{11}$ ($\text{Ln}'\text{Ln}'' = \text{LaY}, \text{LaEr}, \text{LaHo}, \text{and NdDy}$).²⁰ Powder XRD results showed that the $\text{Ln}'\text{Ln}'' = \text{LaY}$ compound adopted an ordered A-site arrangement such that the smaller yttrium ion resides between the basal planes of the Cu–O square pyramids, in the plane of the ordered oxygen vacancies. The smaller lanthanide cation reduces both the distance between the copper–oxygen planes and the in-plane copper–oxygen bond length (with respect to the parent compounds). In YBCO and related cuprates, intercalation of oxygen between the copper sheets is not observed when the small yttrium occupies the cation site between planes. The A-site order in the $\text{Ln}'\text{Ln}'' = \text{NdDy}$ compound could not be ascertained directly from the XRD data (because of the similarity in X-ray scattering factors of the two lanthanides) but was inferred to be similar with the LaY material owing to a similar c/a distortion. Moreover, the copper–oxygen bond lengths, in the NdDy compound, were the smallest in the mixed lanthanide materials, and therefore, this material is a very attractive candidate for realizing superconductivity. We are interested in understanding whether these site-selective substitutions have an effect on the material's defect and chemical properties and their correlations with the normal state and superconducting behavior.

The $\text{Ln}'\text{Ln}''\text{Ba}_2\text{Cu}_2\text{Ti}_2\text{O}_{11}$ materials, with their unique A-site ordering and reduced bond lengths, are therefore very attractive candidates for superconductivity. This communication reports specific variations in the inner architecture to achieve appropriate carrier concentrations and in-situ thermopower and conductivity studies. Both nominally undoped materials, with the stoichiometries $\text{Ln}'\text{Ln}''\text{Ba}_2\text{Cu}_2\text{Ti}_2\text{O}_{11}$ ($\text{Ln}'\text{Ln}'' = \text{LaY}$ and NdDy), and chemically substituted derivatives, $\text{NdDyBa}_{2-x}\text{Sr}_x\text{Cu}_{2+y}\text{Ti}_{2-y}\text{O}_{11}$

(16) Gormezano, A.; Weller, M. T. *Physica C* **1994**, *235–240*, 999–1000.

(17) Gormezano, A.; Weller, M. T. *Chem. Mater.* **1995**, *7*, 1625–1630.

(18) Greenwood, K. B. Ph.D. Thesis, Northwestern University, 1995.

(19) Palacin, M. R.; Casañ-Pastor, N.; Krämer, G.; Jansen, M.; Gómez-Romero, P. *Physica C* **1996**, *261*, 71–80.

(20) Greenwood, K. B.; Sarjeant, G. M.; Poeppelmeier, K. R.; Salvador, P. A.; Mason, T. O.; Dabrowski, B.; Rogacki, K.; Chen, Z. *Chem. Mater.* **1995**, *7*, 1355–1360.

and $\text{La}_{1+x}\text{YBa}_{2-x}\text{Cu}_{2+y}\text{Ti}_{2-y}\text{O}_{11}$, were investigated using equilibrium high-temperature electrical property measurements. The solid solution limits and the effect of high oxygen pressure treatments were investigated. The normal state conductivity and thermopower are reported as a function of oxygen partial pressure, temperature, and composition, and Jonker analyses are used to make comparisons to known superconductors. The electrical property measurements are used to elucidate the internal chemistry of these complex solid state materials.

Experimental Section

Samples were prepared by the solid state reaction of stoichiometric amounts of $\text{LnO}_{1.5}$ ($\text{Ln} = \text{La}, \text{Nd}, \text{Y}, \text{Dy}$), ACO_3 ($\text{A} = \text{Ba}, \text{Sr}$), CuO , and TiO_2 , all of which were of purity above 99.99%. The La_2O_3 was heated at 600 °C for 1 h prior to use to convert any hydroxide back into the oxide, and ACO_3 was annealed in CO_2 at 800 °C to remove hydroxide and nitrate impurities. The reagents were ground and fired in high-density alumina boats at 950 °C in air for 1 day. Each sample was air quenched, ground, and pressed into a pellet several millimeters thick and 0.5 in. in diameter. The pellets were then fired at 1025–1050 °C in air and subsequently quenched, ground, and refired several times during the course of a 3–7 day reaction period. Select samples were subjected to high oxygen pressure treatments in 200 atm of pure oxygen. Annealing temperatures ranged from 650 to 900 °C, with higher temperatures used for phase assemblage investigations and lower temperatures used for oxidation studies of single-phase samples. High oxygen pressure treatments consisted of 24 h anneals at the elevated temperature followed by slow cools, at 0.2 deg/min, to room temperature.

A Rigaku diffractometer with nickel-filtered $\text{Cu K}\alpha$ radiation was employed to collect data on the quenched polycrystalline samples. Phase purity of the samples was ensured by collecting data with a 2θ scan from 15 to 90° with a step of 0.02° and a collection time of 10 s at each step.

Hydrogen reduction thermogravimetry was performed using a Dupont Instruments 951 thermogravimetric analyzer (as previously reported for several quadruple perovskites).^{13,20} Samples were heated at 900 °C in an 8.5% $\text{H}_2/91.5\%$ He atmosphere until an equilibrium weight was established, to reduce the compounds to known components which were identified by an X-ray diffraction trace.

Simultaneous four-point conductivity and thermoelectric coefficient measurements, at temperatures ranging from 650 to 800 °C, were performed using an apparatus described previously.^{13,21} The measured conductivities were corrected to account for the relative density of the specimens (70%–85%).²² Flowing premixtures of oxygen and argon were used to vary the oxygen partial pressure above the sample, from 10^{-5} to 1 atm of oxygen, while the total pressure was maintained at one atmosphere. A Thermox (Pittsburgh, PA) oxygen meter, placed downstream from the sample, was used to confirm the oxygen partial pressure. Measurements were taken only after steady state had been achieved; typical equilibration times were 8–12 h per datum. Prior to removal of the $\text{NdDyBa}_{1.5}\text{Sr}_{0.5}\text{Cu}_{2.2}\text{Ti}_{1.8}\text{O}_{11\pm\delta}$ sample (discussed below), measurements were taken during slow cooling from 800 to 400 °C under pure oxygen at a rate of 20 °C/h.

Temperature-dependent magnetic susceptibility measurements were performed using a Quantum Design Corp. MPMS SQUID susceptometer over the temperature range 5–300 K. Approximately 100 mg of sample (contained in a gelatin capsule) was cooled to 5 K in zero field. Measurements were then taken in a field of 1 T as the sample was heated to 300 K.

Temperature-dependent resistivity measurements were made on select samples, in the range 5–300 K, using a standard four-point measurement technique on bar-shaped specimens ($\approx 10 \times 2 \times 1 \text{ mm}^3$). Electrical contacts were established using silver paint, and measurements were made using current densities in the range 0.1–1 mA/cm².

Results

Stability Ranges and XRD Characterization. Substitutions of both strontium for barium and copper for titanium were

(21) Trestman-Matts, A.; Dorris, S. E.; Mason, T. O. *J. Am. Ceram. Soc.* **1983**, *66*, 589–591.

(22) McLachlan, D. S.; Blaszkiewicz, M.; Newnham, R. E. *J. Am. Ceram. Soc.* **1990**, *73*, 2187–2203.

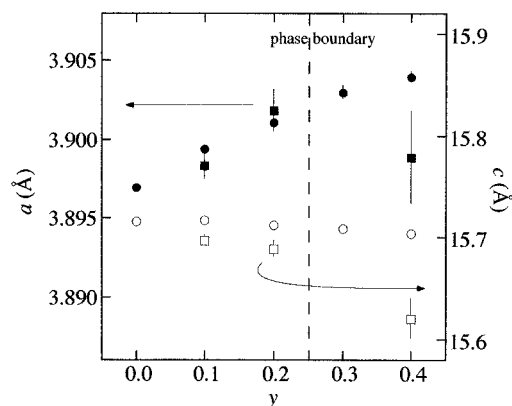


Figure 2. Tetragonal lattice parameters versus substitution level for the $\text{LaYBa}_2\text{Cu}_{2+y}\text{Ti}_{2-y}\text{O}_{11\pm\delta}$ (circles) and $\text{La}_{1+x}\text{YBa}_{2-x}\text{Cu}_{2+y}\text{Ti}_{2-y}\text{O}_{11\pm\delta}$ (squares, $x = y$) compounds. The phase boundary is indicated as a vertical dashed line, a parameters are indicated by filled symbols, and c parameters are indicated by the unfilled symbols.

successful in the $\text{NdDyBa}_{2-x}\text{Sr}_x\text{Cu}_{2+y}\text{Ti}_{2-y}\text{O}_{11\pm\delta}$ system. The substitution of the isovalent strontium for barium was performed to decrease the in-plane copper–oxygen bond lengths, while the substitution of the lower valent copper for titanium was an attempt to increase the copper oxidation state in the CuO_2^{2-} planes. Samples with varying values of x and y ($x = 0.0, 0.5, 1.0$; $y = 0.0, 0.1, 0.2, 0.4$) were characterized for phase purity and lattice parameters with powder XRD. Single-phase samples were attained for $0 \leq x \leq 0.5$, $0 \leq y \leq 0.2$. Samples with higher substitution levels yielded multiphase products, a main phase of the quadruple perovskite, and minor phases which could be identified as $\text{Dy}_2\text{Cu}_2\text{O}_5$, Dy_2O_3 and BaTiO_3 . The $\text{NdDyBa}_{1.5}\text{Sr}_{0.5}\text{Cu}_{2.2}\text{Ti}_{1.8}\text{O}_{11\pm\delta}$ sample has the smallest lattice constant of the phase-pure compositions, with $a = 3.8834(3)$ Å and $c = 15.643(2)$ Å. Compared to those of the parent compound, $\text{NdDyBa}_2\text{Cu}_2\text{Ti}_2\text{O}_{11\pm\delta}$ ($a = 3.8892(2)$ Å and $c = 15.720(2)$ Å),²⁰ the cell contraction is most evident along the c -axis, while a minor decrease in the a -axis is observed.

Replacement of barium and titanium by lanthanum and copper, respectively, was successful in the $\text{La}_{1+x}\text{YBa}_{2-x}\text{Cu}_{2+y}\text{Ti}_{2-y}\text{O}_{11\pm\delta}$ system. Attempts to synthesize strontium-substituted samples, analogous to the NdDy system, were not performed, as the above results (and similar results in the $\text{Gd}_2\text{Ba}_{2-z}\text{Sr}_z\text{Cu}_2\text{Ti}_2\text{O}_{11}$)¹⁸ led to minor decreases in the in-plane lattice constants, while increasing the cationic complexity of the system. Samples with varying values of x and y ($x = 0.0$; $y = 0.0, 0.1, 0.2, 0.4$ and $x = y = 0.0, 0.1, 0.2, 0.4$) were characterized for phase purity and lattice parameters with powder XRD. Single-phase samples were attained for stoichiometries $x = y \leq 0.2$ and $y = 0$; $x \leq 0.2$. (It should be noted that it was difficult to obtain phase pure samples of the $x = 0.0, y = 0.0$ sample reproducibly. In some synthesis attempts, small amounts of unreacted BaTiO_3 were observed as an impurity which did not react even on prolonged annealing.) Samples with higher substitution levels yielded multiphase products with a main phase of the quadruple perovskite. The lattice parameters of the $\text{La}_{1+x}\text{YBa}_{2-x}\text{Cu}_{2+y}\text{Ti}_{2-y}\text{O}_{11\pm\delta}$ systems are displayed in Figure 2, and vary such that the a -axis increases slightly and the c -axis decreases slightly as a function of increasing x and y . The lattice parameters for the solid solution limits are as follows: $x = y = 0$, $a = 3.8969(3)$ Å,²⁰ $c = 15.716(2)$ Å; $x = 0, y = 0.2$, $a = 3.9010(5)$ Å, $c = 15.705(5)$ Å; and $x = 0.2, y = 0.2$, $a = 3.9015(5)$ Å, $c = 15.695(5)$ Å. The a -axis increase is most closely tied to the copper content, as the values in the single-phase region are quite similar for the two substitution schemes, while the c -axis contraction is slightly larger when barium is replaced with the smaller lanthanum

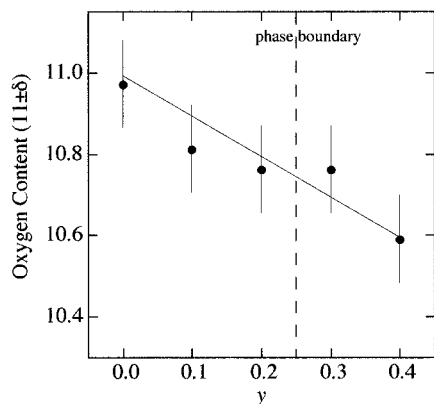


Figure 3. Oxygen content ($11 \pm \delta$) for the $\text{LaYBa}_2\text{Cu}_{2+y}\text{Ti}_{2-y}\text{O}_{11\pm\delta}$ system. The phase boundary is indicated as a vertical, dashed line. Beyond the solubility limit, the doping level and oxygen content have no real meaning for a single phase but are representative of the oxidation state of copper distributed between several phases. The solid line indicates the expected values if all the copper cations are divalent.

cation. A similar effect was observed when the smaller strontium was substituted in the NdDy system (see above).

In both the $\text{NdDyBa}_{2-x}\text{Sr}_x\text{Cu}_{2+y}\text{Ti}_{2-y}\text{O}_{11\pm\delta}$ and the $\text{La}_{1+x}\text{YBa}_{2-x}\text{Cu}_{2+y}\text{Ti}_{2-y}\text{O}_{11\pm\delta}$ systems, it was observed that the overall trends in the lattice parameters continue into the multiphase region. This indicates that the stoichiometry of the main quadruple perovskite phase continues to vary in the multiphase region and that isolation of the more highly substituted phases may be possible under appropriate synthesis conditions. We attempted high oxygen pressure treatments in the multiphase region and were unable to alter the phase assemblage to a discernible extent.

Thermogravimetric Analysis. The oxygen contents of the as-synthesized materials yield the following chemical formulas: $\text{NdDyBa}_2\text{Cu}_2\text{Ti}_2\text{O}_{11.0\pm 0.1}$, $\text{NdDyBa}_{1.5}\text{Sr}_{0.5}\text{Cu}_{2.2}\text{Ti}_{1.8}\text{O}_{10.78\pm 0.1}$, $\text{LaYBa}_2\text{Cu}_2\text{Ti}_2\text{O}_{10.98\pm 0.1}$, $\text{LaYBa}_2\text{Cu}_{2.2}\text{Ti}_{1.8}\text{O}_{10.77\pm 0.1}$, and $\text{La}_{1.2}\text{YBa}_{1.8}\text{Cu}_{2.2}\text{Ti}_{1.8}\text{O}_{10.83\pm 0.05}$. These values correspond to nominally divalent copper in all systems (as synthesized) and indicate that substantial oxidation of the CuO_2^{2-} sheets has not taken place, even upon chemical substitution. Figure 3 illustrates the oxygen content variation as a function of copper doping in the $\text{LaYBa}_2\text{Cu}_{2+y}\text{Ti}_{2-y}\text{O}_{11\pm\delta}$ system. It is important to note that, while the statistical scatter in the experimental thermogravimetric data is too large to accurately address the overall charge state of copper in these materials, these data clearly indicate that oxygen vacancies are an important compensation mechanism when copper is substituted for titanium. Values in the multiphase regions cannot be correlated directly with an oxygen content of the quadruple perovskite phase, owing to the uncertainty in the composition of that phase. However, the thermogravimetric weight loss agrees with divalent copper being reduced to copper metal regardless of the distribution of copper between phases (assuming full oxidation of other cationic species). Similar trends in the oxygen contents have been reported in doping attempts on related quadruple perovskites.^{16,18,19} High oxygen pressure treatments at 900 °C did not significantly alter the lattice parameters or oxygen contents for either the LaY-based or the NdDy-based compounds.

Electrical Characterization and Analysis. In order to more accurately address the overall charge state of copper, in-situ electrical property measurements were conducted. A particularly useful analysis method of thermopower and conductivity data, especially in understanding the internal chemistry of layered cuprates, is the method developed by Jonker.²³ The mathematics of Jonker analysis, and its usefulness for interpret-

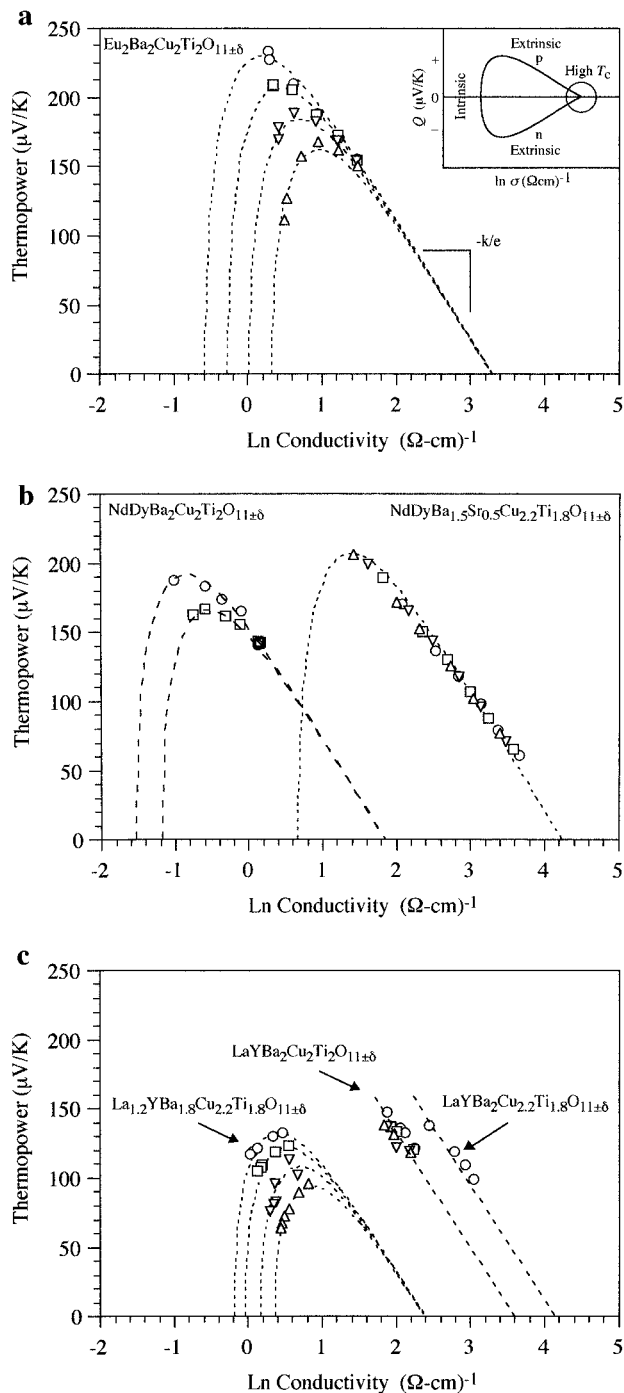


Figure 4. Jonker plots of quadruple perovskites. Insert in part a is a schematic Jonker plot. The region shown by the circle of low thermopower and high conductivity is associated with superconductivity. Symbols correspond to temperatures as follows: $\circ \approx 650$ °C, $\square \approx 700$ °C, $\nabla \approx 750$ °C, and $\triangle \approx 800$ °C. At each temperature, data points correspond to oxygen partial pressures of 10^{-5} , 10^{-4} , 10^{-3} , 10^{-2} , 10^{-1} , and 10^0 atm in a clockwise fashion (unless indicated otherwise): (a) $\text{Eu}_2\text{Ba}_2\text{Cu}_2\text{Ti}_2\text{O}_{11\pm\delta}$, adapted from ref 13; (b) $\text{NdDyBa}_{2-x}\text{Sr}_x\text{Cu}_{2+y}\text{Ti}_{2-y}\text{O}_{11\pm\delta}$; (c) $\text{La}_{1+x}\text{YBa}_{2-x}\text{Cu}_{2+y}\text{Ti}_{2-y}\text{O}_{11\pm\delta}$.

ing electrical properties, are discussed in detail elsewhere.^{13,23,24} Figure 4a–c are plots of the thermopower versus the natural logarithm of the conductivity (Jonker plots) for the systems (a) $\text{Eu}_2\text{Ba}_2\text{Cu}_2\text{Ti}_2\text{O}_{11\pm\delta}$ (data taken from ref 13), (b) $\text{NdDyBa}_{2-x}\text{Sr}_x\text{Cu}_{2+y}\text{Ti}_{2-y}\text{O}_{11\pm\delta}$, and (c) $\text{La}_{1+x}\text{YBa}_{2-x}\text{Cu}_{2+y}\text{Ti}_{2-y}\text{O}_{11\pm\delta}$. The dashed lines through the data for $\text{Eu}_2\text{Ba}_2\text{Cu}_2\text{Ti}_2\text{O}_{11\pm\delta}$ (Figure 4a) are fitted curves based on a two-band semiconductor model,¹³ and these data are included here to

(23) Jonker, G. H. *Philips Res. Rep.* **1968**, *23*, 131–138.

(24) Su, M.-Y.; Elsbernd, C. E.; Mason, T. O. *J. Am. Ceram. Soc.* **1990**, *73*, 415–419.

highlight the salient features of this analysis method. The dashed lines through the remaining data also correspond to the semiconductor model and are included as a guide to the eye. The limited span of the data in the current investigations leads to some uncertainty in the actual curves, and therefore, little emphasis is placed here on the transport parameters calculated from these fits. Of particular importance in analyzing these data, however, with respect to the internal chemistry of materials, is the region of the curve where the data falls and also the spread of the data as a function of the oxygen partial pressure or chemical substitutions. The position of the high conductivity intercept with the zero thermopower axis has interesting physical implications, and empirically observed values of this intercept are strikingly similar for superconducting cuprates (see the Discussion).

The region on the low-conductivity side of the thermopower maximum, having the large positive slope (see the fitted curves in Figure 4a), corresponds to the intrinsic regime (both electrons and holes contribute to the electrical properties). In layered cuprates, this region would correspond to a nominally divalent copper system. Positive values of the thermopower indicate that holes are the majority contributors to the conduction process and that oxidation of the copper–oxygen network is the predominant chemical process. The p-type extrinsic (single carrier) regime corresponds to the linear region on the high-conductivity side of the thermopower maximum, having a slope of $-k/e$ (k is Boltzmann's constant and e is the unit of electronic charge). This slope is labeled in Figure 4a but is equally true for all the plots in Figure 4. As the CuO_2^{2-} planes are oxidized, a transition from intrinsic behavior to hole-doped extrinsic behavior is expected, as has been previously observed in layered cuprates, including the quadruple perovskites. Superconducting compositions display properties in the extrinsic region (heavily doped) with thermopower values below $\approx 40 \mu\text{V/K}$. In addition, deviations from the ideal semiconductor Jonker curve occur, as the thermopower approaches zero in the extrinsic region, owing to a semiconductor-to-metal transition at large doping levels in the layered cuprates. Since the carrier concentration, or oxidized state of the CuO_2^{2-} planes, can be related to the stoichiometry of the material, the position on the curve is dependent on both the oxygen content and cationic composition.

In Figure 4a, the electrical properties are observed to be strong functions of the oxygen partial pressure. Transitions from intrinsic behavior to lightly doped extrinsic behavior are observed as the oxygen partial pressure is increased. In addition, the intrinsic regime becomes more prevalent as the temperature is increased, owing to the thermal generation of carriers across a band gap. These are all consistent with a material which has been slightly oxidized owing to the intercalation of oxygen, but is severely underdoped in relation to the populations where superconductivity is observed.¹³

Both the $\text{NdDyBa}_2\text{Cu}_2\text{Ti}_2\text{O}_{11\pm\delta}$ and $\text{NdDyBa}_{1.5}\text{Sr}_{0.5}\text{Cu}_{2.2}\text{Ti}_{1.8}\text{O}_{11\pm\delta}$ systems (Figure 4b) resemble the $\text{Eu}_2\text{Ba}_2\text{Cu}_2\text{Ti}_2\text{O}_{11\pm\delta}$ system, in that the electrical properties are strong functions of the oxygen partial pressure, but the curves are shifted slightly with respect to the conductivity values. The undoped NdDy system ($T = 650$ and 700°C) exhibits a transition from intrinsic behavior to lightly doped extrinsic behavior as the oxygen partial pressure is increased, as in the Eu system shown in Figure 4a. In addition, the temperature dependence of the electrical properties is in accord with a lightly doped, p-type intrinsic material. The defect species responsible for oxidation, in the europium system, was determined to be interstitial oxygen.¹³ We cannot determine the defect species of the undoped NdDy system unambiguously from the present data, lacking more data in the extrinsic regime. However, the similarity of the crystal

structures and electrical properties of these two systems is strong evidence that the defect structures are similar as well. The overlap of the data at the two different temperatures, in $p\text{O}_2 = 1$ atm (the extrinsic case), is also similar to the undoped Eu system, further suggesting a similar defect structure on the oxygen sublattice.

The doped NdDy system ($\text{NdDyBa}_{1.5}\text{Sr}_{0.5}\text{Cu}_{2.2}\text{Ti}_{1.8}\text{O}_{11\pm\delta}$) exhibits only extrinsic, p-type behavior, where the carrier concentrations are functions of both the temperature and oxygen partial pressure. Thermopowers as low as $60 \mu\text{V/K}$ (at the lowest temperature and highest oxygen partial pressure) demonstrate that the oxidation of the CuO_2^{2-} sheets can be achieved in the quadruple perovskite materials. While the oxygen content analysis indicated that limited oxidation occurred under the synthesis conditions ($T \approx 1050^\circ\text{C}$, $p\text{O}_2 \approx 0.21$ atm), the electrical property measurements demonstrate that carrier concentrations can be increased dramatically by appropriate annealing of specific compositions. Compared to known superconductors, the thermopower values of the doped NdDy system correspond to an underdoped state on the cusp of the region where superconducting materials are observed (thermopower values below $\approx 40 \mu\text{V/K}$). The origin of the dependence of the carrier concentrations on temperature and oxygen pressure is discussed below. The absolute conductivity values are greater in the doped NdDy system than in any of the quadruple perovskites and are similar to those observed for YBCO (see discussion).

The high-temperature electrical properties of the $\text{La}_{1+x}\text{Y}\text{Ba}_{2-x}\text{Cu}_{2+y}\text{Ti}_{2-y}\text{O}_{11\pm\delta}$ system (Figure 4c) contrast those of the Eu or NdDy systems, in that the compositions investigated have electrical properties which are much less dependent on oxygen pressure. This family differs structurally from the materials investigated in Figure 4a,b in that the small yttrium cation preferentially occupies the 8-coordinate A-site between the copper sheets.²⁰ This allows for a contraction of the distance separating the CuO_2^{2-} planes, making oxygen intercalation in this region energetically unfavorable, as reflected in the limited response of the electrical properties to variations in the oxygen partial pressure. $\text{LaYBa}_2\text{Cu}_2\text{Ti}_2\text{O}_{11\pm\delta}$ displays p-type extrinsic behavior with little sensitivity of the thermopower and conductivity to oxygen pressure or temperature. Similar behavior is observed for $\text{YSr}_2\text{Cu}_2\text{GaO}_7$, the parent "undoped" compound of the triple perovskite superconducting family.²⁵ This related compound has a similar structural motif with yttrium residing between the copper–oxygen double sheets. The origin of extrinsic behavior in these undoped materials is undetermined but is likely due to local inhomogeneities or slight deviations from the nominal chemical composition. Similar local inhomogeneities or deviations from nominal stoichiometry are probable explanations for the very weak oxygen pressure dependence of the electrical properties observed for the LaY materials, as well.

$\text{LaYBa}_2\text{Cu}_{2.2}\text{Ti}_{1.8}\text{O}_{11\pm\delta}$ also exhibits p-type extrinsic conductivity and has slightly lower thermopower values than its undoped parent compound, indicating that some electronic compensation (an increase in the carrier concentration on doping) has occurred. This material also has conductivities whose absolute magnitudes are higher than the parent material, as was observed in the doped NdDy system. The thermopower values, however, are not vastly different than the undoped compound, further showing that the substituted copper cations are, to a great extent, self-compensated in these systems (as seen in the thermogravimetric results). Most notably, the copper substitution in $\text{LaYBa}_2\text{Cu}_{2.2}\text{Ti}_{1.8}\text{O}_{11\pm\delta}$, even after low-temperature anneals, does not result in large changes in the carrier

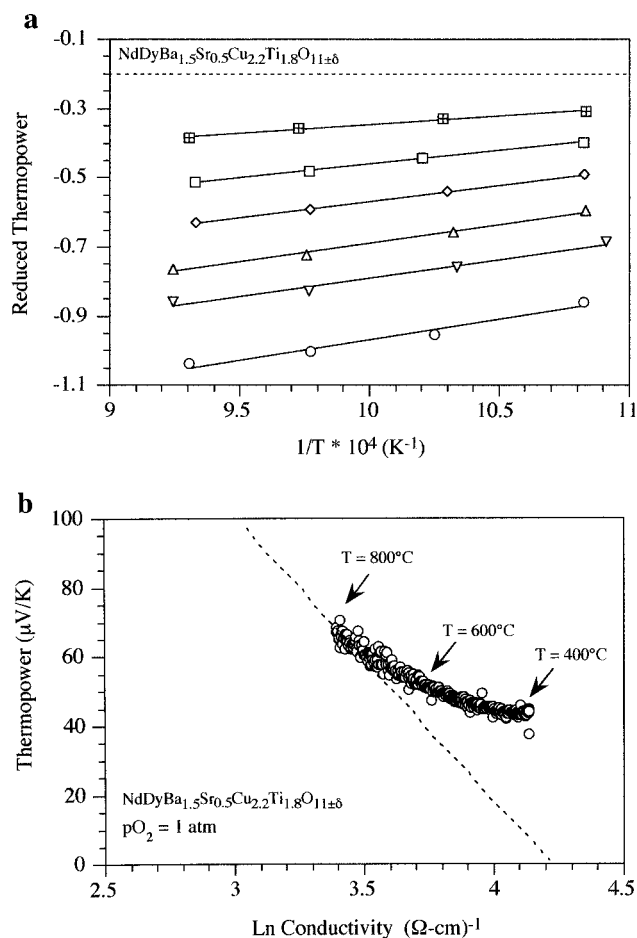


Figure 5. Temperature dependence of the electrical properties for the $\text{NdDyBa}_{1.5}\text{Sr}_{0.5}\text{Cu}_{2.2}\text{Ti}_{1.8}\text{O}_{11\pm\delta}$ system. (a) Reduced thermopower plotted versus inverse temperature. At each temperature, data points correspond to oxygen partial pressures of 10^{-5} , 10^{-4} , 10^{-3} , 10^{-2} , 10^{-1} , and 10^{-0} atm, from lowest to highest reduced thermopower values. (b) Jonker plot of the electrical properties of this system as it was slow cooled ($\approx 20^\circ\text{C/h}$) in pure oxygen. Approximate temperatures are indicated in the illustration.

concentration, in contrast to the observations in the doped NdDy system. Intercalation of oxygen is not observed in the undoped LaY material (as evidenced in the electrical properties) but is observed in the undoped NdDy system, implying that the A-site order, which effects the availability of intercalation pathways, is a significant factor in, and may ultimately control, the oxidation behavior of the blocking layer.

Interestingly, the $\text{La}_{1.2}\text{YBa}_{1.8}\text{Cu}_{2.2}\text{Ti}_{1.8}\text{O}_{11\pm\delta}$ system displays largely intrinsic, p-type behavior. Thus, the cosubstitution of lanthanum for barium and copper for titanium in the nominally undoped compound, which can be regarded as self-compensating if the extra lanthanum and copper are both trivalent, allows the system to move closer to the intrinsic regime (the CuO_2 planes are less oxidized). The $\text{La}_{1.2}\text{YBa}_{1.8}\text{Cu}_{2.2}\text{Ti}_{1.8}\text{O}_{11\pm\delta}$ material can also be considered as a slightly donor doped (La^{3+} for Ba^{2+}) analogue of the $\text{LaYBa}_2\text{Cu}_2\text{Ti}_{1.8}\text{O}_{11}$ material. The donors remove carriers from the system resulting in the observed intrinsic behavior. This transition to the intrinsic regime, resulting from variations in the material's stoichiometry, supports the argument that similar variations in the local chemical composition of the parent compound cause the anomalous p-type extrinsic behavior observed.

The temperature dependence of the electrical properties in the $\text{NdDyBa}_{1.5}\text{Sr}_{0.5}\text{Cu}_{2.2}\text{Ti}_{1.8}\text{O}_{11\pm\delta}$ sample are displayed in Figure 5a,b. In Figure 5a, the thermopower has been converted to a "reduced" thermopower value, Q_R (which is directly proportional to the logarithm of the hole concentration), and

plotted as a function of inverse temperature. The value of the reduced thermopower, Q_R , is given by the following equation, which is valid for extrinsic p-type semiconductors:

$$Q_R = \frac{-eQ}{2.303k} = \log p - \log N^+ + \frac{A^+}{2.303} \quad (1)$$

where p is the concentration of holes, N^+ is the density of states in the valence band, and A^+ is a transport constant for holes with a value between 0 and 2.²⁶ As observed in Figure 5a, at any given oxygen pressure, the carrier concentrations increase as the temperature is decreased (assuming the density of states and transport coefficient are temperature-independent). This behavior is in contrast to the temperature-independent behavior observed in the extrinsic region of the related quadruple perovskites, $\text{La}_2\text{Ba}_2\text{Cu}_2\text{Ti}_2\text{O}_{11}$ and $\text{Eu}_2\text{Ba}_2\text{Cu}_2\text{Ti}_2\text{O}_{11}$,¹³ but is similar to that observed in the YBCO materials. The enthalpies of oxidation, or generation of holes, in the former systems were shown to be near zero, while the enthalpy of the doped NdDy system varies as a function of the oxygen partial pressure. Values between -0.23 and -0.10 eV ($p\text{O}_2[\text{atm}]/\Delta H_{\text{ox}}[\text{eV}]$: $10^{-5}/-0.23$, $10^{-4}/-0.21$, $10^{-3}/-0.21$, $10^{-2}/-0.18$, $10^{-1}/-0.13$, $10^0/-0.10$) were derived from the data shown in Figure 5a. Since the composition must be changing as a function of temperature and oxygen partial pressure, leading to the observed dependencies of the carrier concentrations in the extrinsic regime, the enthalpy of oxidation must be composition-dependent in the NdDy material. The difference between the undoped parent compounds and the doped analogue can be explained by the filling of different oxygen sites in the two cases and is discussed further below.

Figure 5b is a Jonker plot of data collected as the sample was slow cooled in 1 atm of oxygen and shows that thermopowers as low as $40 \mu\text{V/K}$ are attainable in this system. Also noticeable in this analysis is the deviation, at the lowest thermopower values, from linear behavior. The straight line, in Figure 5b, is the slope expected for an extrinsic semiconductor and the deviation toward higher conductivity values is consistent with a semiconductor to metal transition. Resistivity measurements at low temperatures confirm a decreased resistivity with decreasing temperature ($\rho^{T=300\text{K}} = 8 \text{ m}\Omega \text{ cm}$, $\rho^{T=100\text{K}} = 7 \text{ m}\Omega \text{ cm}$), consistent with metallic behavior in this highly doped material.

Magnetic Characterization. The temperature-dependent magnetic susceptibility of select samples, quenched from 1050°C in air, in the $\text{La}_{1+x}\text{YBa}_{2-x}\text{Cu}_{2+y}\text{Ti}_{2-y}\text{O}_{11\pm\delta}$ system are shown in Figure 6 (Note that the $x = 0.4$, $y = 0.4$ and $x = 0.0$, $y = 0.3$ samples not pure phase, as was discussed above). An antiferromagnetic transition ($\approx 13 \text{ K}$), typical of lightly doped layered cuprates (the parent phases of superconductors) is observed in several of the samples. As carrier doping increases we expect the antiferromagnetic response to become weaker, if these materials behave similarly to the high- T_c cuprates. The data in Figure 6 suggests that carrier concentrations increase, in the $\text{LaYBa}_2\text{Cu}_{2+y}\text{Ti}_{2-y}\text{O}_{11\pm\delta}$ system, as y is increased. In fact, the magnetic behaviors of the $x = 0$, $y = 0.2/0.3$ samples show no evidence of an antiferromagnetic transition. The cosubstituted samples, $\text{La}_{1+x}\text{YBa}_{2-x}\text{Cu}_{2+y}\text{Ti}_{2-y}\text{O}_{11\pm\delta}$ $x = y = 0.2/0.4$, have the strongest antiferromagnetic response of the samples investigated, suggesting that the carrier concentration decreases on cosubstitution. The trends in the carrier concentration observed in both the SQUID measurements and thermopower measurements agree well. SQUID data on the NdDy samples are similar in nature to the LaY samples but are not included owing to the strong compositional effects that variations in the annealing/

(26) Ioffe, A. F. *Physics of Semiconductors*; Infosearch Limited: London, 1960.

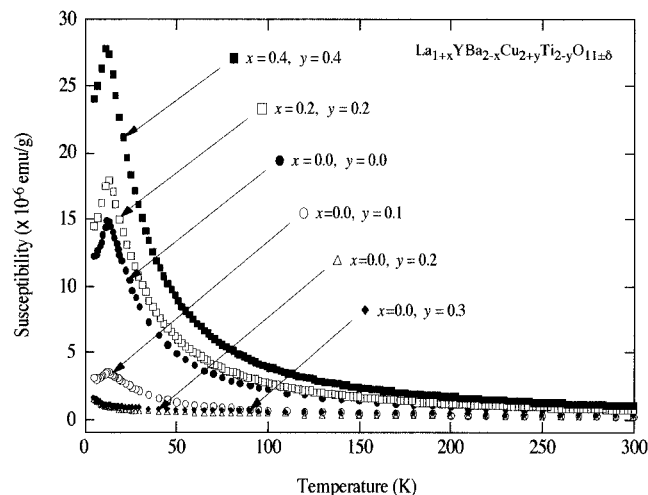


Figure 6. Temperature-dependent magnetic measurements (χ vs T) of select samples (as indicated in illustration) in the $\text{La}_{1+x}\text{YBa}_{2-x}\text{Cu}_{2+y}\text{Ti}_{2-y}\text{O}_{11\pm\delta}$ system, quenched from 1050 °C in air.

quenching procedures have in this system. However, no evidence for diamagnetism (or superconductivity) was observed in the slow cooled samples exhibiting metallic-like conductivity.

Discussion

The primary result of these investigations is that oxidation of the copper–oxygen planes is possible in these systems, whose transport properties are remarkably similar to known superconductors, but is highly dependent on other aspects of the internal chemistry, such as the intercalation behavior, defect chemistry, and solid solution limits. Solid solutions of cations were observed in the present work over several sites in the quadruple perovskite structure: copper for titanium, strontium for barium, and simultaneous replacement of lanthanum for barium and copper for titanium. However, both thermogravimetric oxygen content data and thermopower measurements indicate that oxidation is minimal in the as-synthesized materials. This behavior is consistent with that presented in other reports concerning the quadruple perovskites.^{15,16,18,19} In contrast, attempts to substitute alkaline earths for lanthanide cations were unsuccessful in maintaining single-phase quadruple perovskites, or doping carriers into the system, but led to the formation of new members of the layered perovskite family, all of which have nominally divalent copper.²⁷

The ability for solid solutions to exist in this structure is to one degree controlled by the site preference of the substituted cations but to a greater degree by the ability of the structure to accommodate the substituted cations and maintain a 2+ oxidation state of copper (or more generally, a 2− overall charge in the CuO_2 planes). The preference of copper for the divalent state in the quadruple perovskites, under the synthesis conditions employed here and in previous work, is a major chemical factor which leads to the observed stable solid solutions. Thus, isovalent or self-compensating solid solutions are most successful and more widely observed, in the quadruple perovskites, than electronically compensated aliovalent substitutions (which might lead to superconductivity).

Isovalent substitutions of both strontium for barium, as observed in this work, tin for titanium,² or various lanthanide substitutions^{2–6,13,15–20,28} have extensive solid solution ranges. Additionally, marked solubilities exist for aliovalent substitutions (i.e., Sc^{+3} , Cu^{+2} , Co^{+3} , Al^{+3} , Ga^{+3}) on the titanium site, with

(27) Otzsch, K. D.; Poepfelmeier, K. R.; Salvador, P. A.; Mason, T. O.; Zhang, H.; Marks, L. D. *J. Am. Chem. Soc.* **1996**, *118*, 8951–8952.

(28) Gómez-Romero, P.; Palacín, M. R.; Rodríguez-Carvajal, J. *Chem. Mater.* **1994**, *6*, 2118–2122.

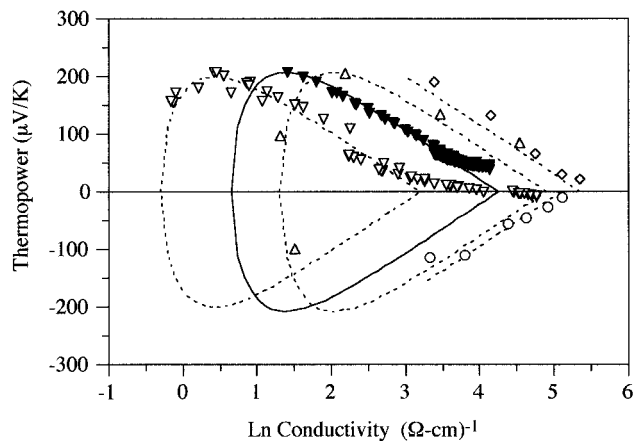


Figure 7. Comparative Jonker plot of the $\text{NdDyBa}_{1.5}\text{Sr}_{0.5}\text{Cu}_{2.2}\text{Ti}_{1.8}\text{O}_{11\pm\delta}$ sample (\blacktriangledown) and several known superconducting layered cuprates: (∇) $\text{Bi}_{2.1}\text{Sr}_{1.9}\text{Ca}_{1-x}\text{Y}_x\text{Cu}_2\text{O}_y$ (after ref 29); (\triangle) $\text{YBa}_2\text{Cu}_3\text{O}_{7-x}$ (after ref 24); (\circ) $\text{Nd}_{2-x}\text{Ce}_x\text{Cu}_2\text{O}_4$ (after ref 31); (\diamond) $\text{La}_{2-x}\text{Ba}_x\text{Cu}_2\text{O}_{4\pm\delta}$ (after ref 31). Dashed lines are fitted Jonker curves from the prior investigations, and the solid line is the fitted curve from the present investigation.

a concomitant decrease in the observed oxygen content.^{15,16,18,19} The ability of the structure to self-compensate the acceptor dopants by oxygen vacancies, rather than holes, apparently stabilizes these solid solutions. With titanium in the blocking layer, which has a strong preference to maintain octahedral coordination, acceptor substitutions on the A site are energetically unstable owing to the inflexibility of the structure to alter its oxygen content and preserve the coordination environments of the constituent A and B cations. Owing to the ability of B-site acceptor dopants, such as copper, cobalt, gallium, etc., to adopt coordination numbers less than 6, increased solid solubilities are possible without extensive oxidation of the copper–oxygen sheets (however, more accurate studies of the structural location of oxygen vacancies are warranted). Similarly, the ability of lanthanum to substitute on the barium site is made possible when copper is simultaneously substituted on the titanium sites, leading to a self-compensated doping scheme. This cosubstitution allows the material to remain in its preferred electronic state, while demonstrating the ability for substantial aliovalent substitutions on the A site of the quadruple perovskite.

The arguments presented above for the stability of non-oxidized copper–oxygen planes, under standard synthesis conditions, require us to pursue alternate methods for oxidation of these compounds. One alternative method to increase carrier concentrations has been demonstrated in the quadruple perovskites, as evidenced in the electrical properties and magnetic measurements (Figures 5 and 6), through self-compensated cationic substitutions and subsequent reoxidation at low temperatures. This behavior is similar to that observed in YBCO, where low-temperature oxidation is required to increase the oxygen concentration and optimize superconductivity. Several important similarities of the transport properties exist between the YBCO system, as well as other superconducting layered cuprates, and the copper-substituted NdDy system. Figure 7 is a comparison of Jonker plots for several known superconductors and the substituted NdDy system of the present study. The substitution of copper for titanium in the quadruple perovskites shifts the upper intercept of the Jonker curve (which is related to the density of states–mobility product^{13,23,24}) toward higher conductivities (see Figure 4). The similarity of this value for the substituted NdDy material and known superconductors is strong evidence that control over the internal chemistry of the quadruple perovskites should ultimately lead to superconductiv-

ity. The $\text{Bi}_{2-x}\text{Sr}_{1.9}\text{Ca}_{1-x}\text{Y}_x\text{Cu}_2\text{O}_y$ (BSCCO)²⁹ and $\text{YSr}_2\text{Cu}_2\text{GaO}_7$ ³⁰ systems, which have intercepts for the underdoped materials at low conductivities, display large deviations upon doping, and superconducting compositions lie in the range $\ln \sigma \approx 4-6$.^{24,30} The quadruple perovskites display a similar excursion for highly substituted systems, as illustrated in Figure 7. This excursion could be due to a highly degenerate semiconductive state or a metallic transition in the quadruple perovskite. Low-temperature resistivity measurements indicate that a metallic transition does occur in the doped quadruple perovskites, further evidence that the carrier concentrations have been substantially increased.

Despite the large increase in copper content in the quadruple perovskites, which could lead to extrinsic, acceptor-doped behavior, the oxygen pressure dependence of the electrical properties remains an essential chemical feature. The temperature dependence observed in Figure 5 for the substituted NdDy compound contrasts that of the unsubstituted quadruple perovskites, where no temperature dependence was observed in the extrinsic region. This implies that oxidation in the substituted system occurs via a different mechanism than that observed in the parent compounds. A plausible explanation of these data is that, rather than filling the vacant oxygen sites between the copper-oxygen planes as observed in the parent stoichiometric compounds, the extra oxygen vacancies in the blocking layer (introduced as a compensation to the copper substitution) are being filled in the substituted compound. This oxidation mechanism would leave the doped copper-oxygen sheets unperturbed and favor superconductivity. Ultimately, increased filling of these blocking layer oxygen vacancies would lead to a temperature-dependent behavior more similar to that of the parent compound, owing to the decreasing number of vacant oxygen sites. Thus, the enthalpy is observed to increase as the oxygen sites become filled. A similar Jonker behavior is observed in the YBCO system,³¹ where the chain site oxygen content is known to be dependent on the temperature and oxygen pressure.³² The introduction of copper in the blocking layer of the present quadruple perovskite imparts behavior reminiscent to that of the triple perovskite YBCO system. While these arguments qualitatively explain the observed data, direct investigations of the structural location of oxygen defects are necessary to confirm this model, and neutron diffraction experiments are currently underway.

The absence of reoxidation in the doped LaY materials is somewhat surprising. We have shown that the fast oxygen intercalation pathway between the copper planes has been removed by the structural position of the small yttrium cation. This is evidenced by the behavior of the electrical properties in the undoped case. We might expect that the thermodynamic state of the doped LaY material should be an oxidized copper-oxygen network, as observed in the NdDy case at low temperatures. However, this is not observed experimentally. The doped LaY compound has little response to oxygen partial pressure variations. Thus, the A-site chemical architecture is

(29) Hong, B.-S.; Mason, T. O. In *Point Defects and Related Properties of Ceramics*; Mason, T. O., Roubort, J. L., Eds.; American Ceramic Society: Westerville, OH, 1991; pp 292-301.

(30) Tomlins, G. W.; Jeon, N.-L.; Mason, T. O.; Groenke, D. A.; Vaughney, J. T.; Poepelmeier, K. R. *J. Solid State Chem.* **1994**, *109*, 338-344.

(31) Su, M.-Y.; Elsbernd, C. E.; Mason, T. O. *Physica C* **1989**, *160*, 114-118.

(32) Kishio, K.; Shimoyama, J.-I.; Hasegawa, T.; Kitazawa, K.; Fueki, K. *Jpn. J. Appl. Phys.* **1987**, *26*, 1228-1230.

(33) Shen, L.; Salvador, P. A.; Mason, T. O. *J. Phys. Chem. Solids* **1996**, *57*, 1311-1319.

(34) Hong, B.-S.; Mason, T. O. In *Superconductivity and Ceramic Superconductors II*; Nair, K. M., Balachandran, U., Chiang, Y.-M., Bhalla, A. S., Eds.; American Ceramic Society: Westerville, OH, 1991; Vol. 18, pp 95-106.

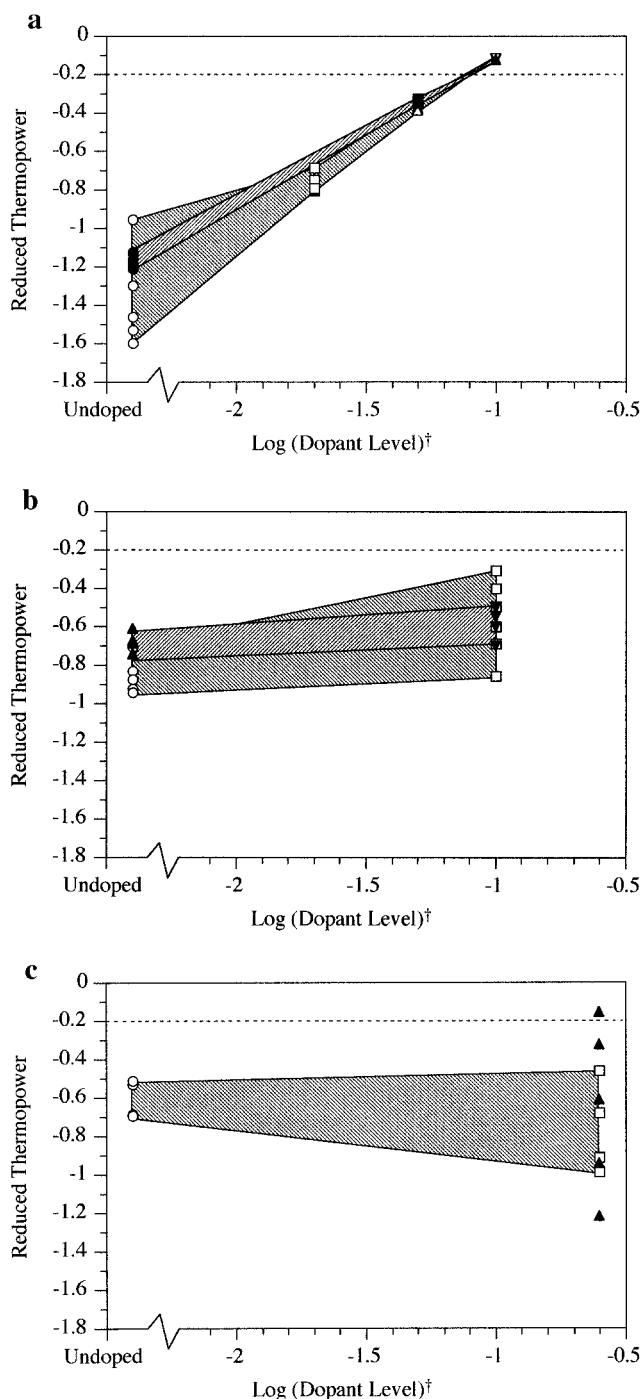


Figure 8. Reduced thermopower versus the logarithm of the dopant concentration for several layered cuprates at $T \approx 650$ °C, except where noted. The dopant concentration is defined as the number of aliovalent substitutional cations per copper plane (see text) and is listed [in brackets] below for each material: (a) $\text{La}_{2-x}\text{Ca}_x\text{CuO}_{4\pm\delta}$ [x], unfilled symbols, $T \approx 700$ °C, adapted from ref 33 and $\text{Y}_{1-x}\text{Ca}_x\text{Sr}_2\text{Cu}_2\text{GaO}_7$ [$x/2$], filled symbols, $T \approx 750$ °C, adapted from ref 30; (b) $\text{NdDyBa}_2\text{Cu}_{2+y}\text{Ti}_{2-y}\text{O}_{11\pm\delta}$ [$y/2$], unfilled symbols and $\text{LaYBa}_2\text{Cu}_{2+y}\text{Ti}_{2-y}\text{O}_{11\pm\delta}$ [$y/2$], filled symbols; (c) $\text{La}_{1.5-x}\text{Ba}_{1.5+x}\text{Cu}_3\text{O}_{7\pm\delta}$ [$x/2$], unfilled symbols, adapted from ref 34 and $\text{YBa}_2\text{Cu}_3\text{O}_{7-\delta}$ [0.25], filled symbols, adapted from ref 24. At each dopant level, for a given system, different data points correspond to changes in the oxygen partial pressure.

directly influencing the internal chemistry. Either there is a kinetic stabilization of the underdoped state in the copper-substituted LaY compound or there is truly a thermodynamic difference in the oxidation behavior of these two systems.

Kinetic stabilization would lead to slow equilibration times and constant drift in the experimental data, but these features were not observed experimentally. Anneals in air at 700 °C

for several days did not result in an increased carrier concentration (oxidation). What is surprising is that, at 1050 °C, oxygen vacancies were incorporated into the structure, but at 700 °C, these vacancies cannot be refilled. Both the longer copper–oxygen bond lengths and the inability of oxygen to reside in the plane between the copper oxygen planes in the LaY system could lead to a thermodynamic stability of the lightly doped case. Further experiments are required to understand whether longer bond lengths, dissimilar oxygen vacancy arrangements, or kinetic factors stabilize underdoped case in the LaY.

Further attention on the long bond lengths in these quadruple perovskites is warranted, owing to the previous emphasis on these values as an explanation for the absence of superconductivity in the quadruple perovskites. The current study suggests that the long bond lengths act as a barrier to oxidation under standard synthesis conditions. In air at 1050 °C, all samples have low carrier concentrations. Oxidation is observed for materials with the smallest in-plane bond lengths studied, which are still slightly longer than known superconductors, when annealed at low temperatures and high oxygen partial pressures. An important distinction must be made between the absence of superconductivity owing to long bond lengths and the absence of oxidation owing to long bond lengths. While the latter necessarily results in the former, oxidation may be achieved through novel approaches to the synthesis of electronically compensated materials. As for the current study, one plausible explanation is that the absence of reoxidation of the doped LaY material results from the longer in-plane bond lengths, as compared to the oxidized NdDy system. Neutron diffraction studies which investigate the structural location of the oxygen vacancies in these doped systems are warranted.

The potential for superconductivity in the quadruple perovskites can be further demonstrated by focusing on the reduced thermopower values versus nominal doping compositions. Figure 8 compares these values of the LaY and NdDy materials, shown in Figure 8b, with those of other layered cuprates: $\text{La}_{2-x}\text{Ca}_x\text{CuO}_{4\pm\delta}$ (Ca-214) and $\text{Y}_{1-x}\text{Ca}_x\text{Sr}_2\text{Cu}_2\text{GaO}_7$ (Ca-gallate) in Figure 8a and $\text{La}_{1.5-x}\text{Ba}_{1.5+x}\text{Cu}_3\text{O}_{7\pm\delta}$ (LBCO) and $\text{YBa}_2\text{Cu}_3\text{O}_{7-\delta}$ (YBCO) in Figure 8c. In all cases, the doping level has been normalized (see caption) to the number of copper layers per formula unit. In addition, the doping level in the quadruple perovskite was fixed assuming that the substituted copper is trivalent (corresponding to the lower doping limit). Thus, a substitution level of 0.2 coppers in the quadruple perovskites corresponds to a doping level of 0.1. The data at each doping level contain values from several different oxygen partial pressures, where the highest oxygen pressure (1 atm) always corresponds to the highest reduced thermopower value. Schematic bands of oxygen pressure response have been included in the figure to emphasize different oxidation mechanisms in layered cuprates.

Both the doped Ca-214 and Ca-gallate systems have limited responses to the oxygen partial pressure but dramatic responses to the substitution of aliovalent cations. The linear relationship between the logarithm of the normalized dopant level and the reduced thermopower illustrates that oxidation occurs as a direct result of aliovalent substitutions. Furthermore, the overlap of the data of these two structurally distinct systems indicates that the underlying transport properties are similar in layered cuprates. Superconductivity is observed at the normalized doping level of 0.1 (and above) in these two systems. Thus, a

dashed-horizontal line has been included on all plots in Figure 8, at a reduced thermopower value of -0.2 , which is an approximate value above which superconductivity may be expected. In contrast to the behavior observed in Figure 8a, the NdDy quadruple perovskites (Figure 8b) and the YBCO and LBCO systems (Figure 8c) have little sensitivity to the dopant level, but strong responses to the oxygen partial pressure. The YBCO system is the only sample which has a reduced thermopower above -0.2 under these annealing conditions. Interestingly, the LaY materials behave similarly to the Ca-gallate with respect to their oxygen pressure dependencies (compressed responses) but have little dependence on the substitution level, unlike the superconducting gallate. Most importantly, the doped quadruple perovskite demonstrates that, with appropriate synthesis and annealing conditions, the carrier concentrations in the CuO_2 planes can be increased to the threshold of superconducting levels. These materials show metallic-like behavior in this underdoped state. The chemical results described herein demonstrate that a combination of novel synthesis and/or annealing methods which allow for both increased substitution levels and carrier concentrations should lead to superconductivity in this family of materials and is being pursued.

Conclusions

The chemical solubilities, evolution of lattice parameters, as-synthesized oxygen contents, in-situ equilibrium electrical behavior, and low-temperature magnetic behavior of the $\text{NdDyBa}_{2-x}\text{Sr}_x\text{Cu}_{2-y}\text{Ti}_{2+y}\text{O}_{11\pm\delta}$ and $\text{La}_{1+x}\text{YBa}_{2-x}\text{Cu}_{2+y}\text{Ti}_{2-y}\text{O}_{11\pm\delta}$ systems have demonstrated that the relationship between the internal chemistry and inner architecture of the quadruple perovskite family of layered cuprates is directly related to their macroscopic physical properties. The electronic stability of lightly oxidized CuO_2^{2-} sheets has been shown to be an important factor which controls the solid solubilities of different cationic species. The exclusion of interstitial oxygen defects, an important step toward achieving superconductivity by preserving the structural integrity of the CuO_2^{2-} planes, has been demonstrated in the $\text{LaYBa}_2\text{Cu}_2\text{Ti}_2\text{O}_{11}$ -based materials. However, oxidation of this family is observed to be more difficult than the related $\text{NdDyBa}_2\text{Cu}_2\text{Ti}_2\text{O}_{11}$ system. Oxidation of the latter compound has been achieved, another important step toward achieving superconductivity, and an underdoped metallic behavior reminiscent of known superconductors has been observed. While oxygen vacancies play a role in both the undoped and doped NdDy materials, the temperature-dependent population of these defects argues that different types of oxygen defects are present in the two cases. Post-filling of the structural vacancies introduced on synthesis, to compensate the acceptor dopants, is an effective means of oxidation in the NdDy system.

Acknowledgment. This work was supported by the National Science Foundation (Award No. DMR-91-20000) through the Science and Technology Center for Superconductivity and made use of MRL Central Facilities supported by the National Science Foundation, at the Materials Research Center of Northwestern University (Award No. DMR-9120521). K.O. is partly supported by a Research Fellowship of the Japan Society for the Promotion of the Science for Young Scientists.

JA963908R